A Simple and Complete Discrete Exterior Calculus on General Polygonal Meshes

LENKA PTACKOVA, IMPA, lenka@impa.br
LUIZ VELHO, IMPA, lvelho@impa.br

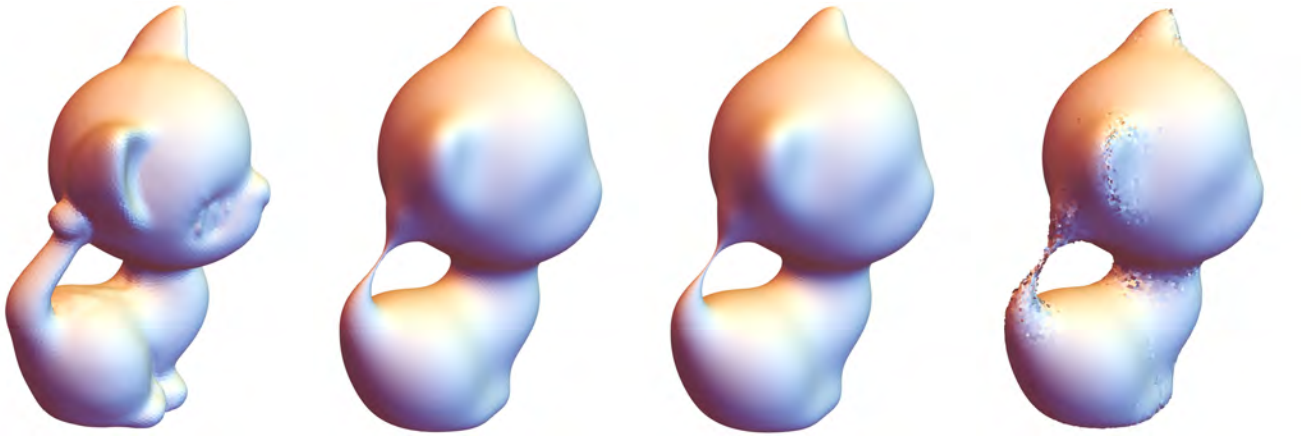

Fig. 1. Comparison of implicit mean curvature flows on a general polygonal mesh (29k vertices) after 10 iterations with time step $t = 10^{-4}$. On the far left is the original mesh. Our method (second from left) and the the algorithm of [M. and M. 2011] with $\lambda = 1$ (third from left) produce a visually well–smoothed meshes. However, the method of [M. and M. 2011] with $\lambda = 0$ (far right) exhibits some undesirable artifacts on the ears, neck, and tail of the kitten.

Discrete exterior calculus (DEC) offers a coordinate-free discretization of exterior calculus especially suited for computations on curved spaces. In this work, we present an extended version of DEC on surface meshes formed by general polygons that bypasses the need for combinatorial subdivision and does not involve any dual mesh. At its core, our approach introduces a polygonal wedge product that is compatible with the discrete exterior derivative in the sense that it satisfies the Leibniz product rule. Based on the discrete wedge product, we then derive a novel primal–to–primal Hodge star operator. Combining these three 'basic operators' we then define discrete versions of the contraction operator and Lie derivative, codifferential and Laplace operator. We discuss the numerical convergence of each one of these operators and compare them to existing DEC methods. Finally, we show simple applications of our operators on Helmholtz–Hodge decomposition, Laplacian surface fairing, and Lie advection of functions and vector fields on meshes formed by general polygons.

CCS Concepts: • **Computing methodologies** → **Mesh models**; **Mesh geometry models**; *Shape modeling*; *Shape analysis*;

Additional Key Words and Phrases: Polygonal meshes, discrete exterior calculus, discrete differential geometry, polygonal wedge product, polygonal Hodge star operator, discrete Laplacian, discrete Lie derivative, discrete Helmholtz–Hodge decomposition, discrete Lie advection.

Authors' addresses: Lenka Ptackova, IMPA, Estr. Dona Castorina, 110 - Jardim Botanico, Rio de Janeiro, Brazil, lenka@impa.br; Luiz Velho, IMPA, Estr. Dona Castorina, 110 - Jardim Botanico, Rio de Janeiro, Brazil, lvelho@impa.br.

Reference Format:
Lenka Ptackova and Luiz Velho. 2018. A Simple and Complete Discrete Exterior Calculus on General Polygonal Meshes. 12 pages. http://w3.impa.br/~lenka

1 INTRODUCTION

The discretization of differential operators on surfaces is fundamental for geometry processing tasks, ranging from remeshing to vector fields manipulation. Discrete exterior calculus (DEC) is arguably one of the prevalent numerical frameworks to derive such discrete differential operators. However, the vast majority of work on DEC is restricted to simplicial meshes, and far less attention has been given to meshes formed by arbitrary polygons, possibly non–planar and non–convex.

In this work, we propose a new discretizaton for several operators commonly associated to DEC that operate directly on polygons without involving any subdivision. Our approach offers three main practical benefits. First, by working directly with polygonal meshes, we overcome the ambiguities of subdividing a discrete surface into a triangle mesh. Second, our construction operates solely on primal elements, thus removing any dependency on dual meshes. Finally, our method includes the discretization of new differential operators such as the contraction and Lie derivatives.

We concisely expose our framework, describe each of our operators and compare them to existing DEC methods. We examine the accuracy of our numerical scheme by a series of convergence tests on flat and curved surface meshes. We also demonstrate the applicability of our method for Helmholtz–Hodge decomposition

of vector fields, surface fairing, and Lie advection of vector fields and functions.

1.1 Contributions and Overview

In the following sections, we focus on the main concepts and properties of proposed operators, compare them to existing DEC schemes, and provide some simple applications of our methods.

- In Section 2 we briefly present related work, talk about basic notions, and discuss the main differences between our concept and the approach of previous research in the area.
- We define a new discrete wedge product on polygonal meshes and show experimental convergence of the product of two discrete forms to the continuous wedge product of respective differential forms in Section 3.1.
- We then provide a novel primal–primal discretization of the Hodge star operator (Section 3.2) that is compatible with the discrete wedge product. Using these two operators we derive a discrete inner product in Section 3.3.
- Employing the discrete Hodge star and wedge product we define a discrete contraction operator (Section 3.4). We then use the Cartan's magic formula to derive a discrete Lie derivative and discuss its convergence to the continuous version in Section 3.5.
- In Section 3.6 we define and examine a novel discrete codifferential operator on polygonal meshes and next a discrete Laplace operator in Section 3.7.
- We illustrate the application of our operators in mesh smoothing (Section 4.1), Helmholtz–Hodge decomposition (Section 4.2), and Lie advection of vector fields (Section 4.3).
- We conclude and suggest future work in Section 5.

2 RELATED WORK AND PRELIMINARIES

There is a vast literature on discrete exterior calculus on triangle meshes, e.g., [K. et al. 2013; M. et al. 2006, 2005; N. 2003] – all these publications have in common that they deal with purely simplicial meshes and use a dual mesh to define operators, we will refer to their approach as to the **classical DEC** from now on.

As announced, unlike the classical DEC, our method works with general polygonal meshes and does not involve any dual meshes. However, our operators differ also in other aspects, e.g., support domains. Next we briefly introduce several basic DEC notions and point out the key differences of our approach compared to existing schemes, principally to the classical DEC.

2.1 Discrete differential forms and the exterior derivative

We strictly stick to the convention, common to previous DEC literature, that a discrete q–form is located on q–dimensional cells of the given mesh.

Discrete differential forms are usually denoted by small Greek letters and sometimes we add a number superscript to emphasize the degree of the form, i.e., a q–form α can be denoted as α^q. The group of all discrete forms of a degree q of a given mesh S is denoted by $C^q(S)$.

A polygonal mesh S is made of a set of vertices (0–dimensional cells), edges (1–dimensional cells), and faces (2–dimensional cells). A real discrete differential q–form α^q on S is a q–cochain, i.e., a real number assigned to each q–dimensional cell c^q of S. E.g., if $(e_0, e_1, \ldots, e_n)$ is the vector of all edges of S, then an 1–form α^1 is a vector of real values

$$\alpha^1 = (\alpha(e_0), \ldots, \alpha(e_n)).$$

The **discrete exterior derivative** d is the coboundary operator and it holds:

$$(d\alpha)(c^{q+1}) = \alpha(\partial c^{q+1}) = \sum_{c^q \in S} [c^{q+1} : c^q]\alpha(c^q),$$

where ∂ denotes the boundary operator and $[c^{q+1} : c^q]$ denotes the incidence relation between cells c^{q+1} and c^q. See an example bellow.

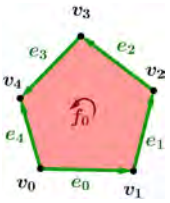

$$[f_0 : e_0] = 1, [f_0 : e_1] = 1, \ldots, [f_0 : e_4] = -1$$

$$\partial f_0 = \sum_{e_i \in S} [f_0 : e_i] e_i = e_0 + e_1 + e_2 + e_3 - e_4$$

$$\alpha^1 = (\alpha(e_0), \ldots, \alpha(e_n))$$

$$d\alpha(f_0) = \sum_{e_i \in S} [f_0 : e_i]\alpha(e_i)$$

$$= \alpha(e_0) + \alpha(e_1) + \alpha(e_2) + \alpha(e_3) - \alpha(e_4)$$

In the figure above, the boundary of the face f_0 is a sum of incident oriented edges, where we take in account the orientation of the bounary edges wrt to the given face. The discrete exterior derivative of a 1–form α^1 (that is stored on edges) is a 2–form $d\alpha$ located on faces and on the face f_0 it is the "oriented sum" of the values of α on boundary edges of f_0.

2.2 The cup product and the wedge product

Since we consider the wedge product on polygons to be the main building block of our theory, we enjoy the opportunity to ponder about it here.

On smooth manifolds, the wedge product allows for building higher degree forms from lower degree ones. Similarly in algebraic topology of pseudomanifolds, a cup product is a product of two cochains of arbitrary degree p and q that returns a cochain of degree $p+q$ located on $(p+q)$–dimensional cells. Thus we consider the cup product to be the appropriate discrete version of the wedge product.

The cup product was introduced by J. W. Alexander, E. Čech, and H. Whitney [H. 1957] in 1930's and it became a well–studied notion in algebraic topology, mainly in the simplicial setting. Later, the cup product was extended also to n–cubes [F. 2012; Massey 1991].

In graphics, Gu and Yau [X. and S.-T. 2003] presented the definition of a wedge product of two discrete 1–forms on triangulations, which turns to be equivalent to the cup product of two 1–cochains on triangle complexes well studied in algebraic topology [H. 1957].

Our discrete wedge product is equivalent to the cup product of [H. 1957] on triangles, and thus to the discrete wedge product of two 1–forms of [X. and S.-T. 2003] on triangles, see also the Figure 2. Furthermore, our discrete wedge product is equivalent to the cup product of [F. 2012; Massey 1991] on quadrilaterals.

In [R. et al. 2011a,b] the authors also studied the cup product on cubical and general polyhedral complexes P, but they employed the so called AT–model, an algebraic set of data that provides homological information about the the underlying complex P.

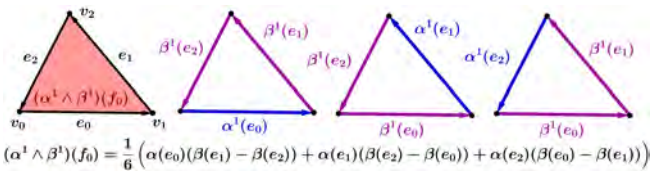

Fig. 2. The wedge (cup) product of two 1–forms (1–cochains) on a triangle: the product of two 1–forms is a 2–form located on faces (far left).

In common to previous approaches, this notion of discrete wedge product is metric–independent and satisfies core properties such as the Leibniz product rule, skew–commutativity, and associativity on closed forms.

Alternative metric–dependent versions of the discrete wedge product on simplicial complexes were suggested in [N. 2003, Section 7.2]. In particular, specialized expressions were necessary to address the different combination of primal and dual forms.

2.3 The Hodge star operator

The most common discretization of the Hodge star operator on triangle meshes is the so called diagonal approximation, which is computed based on the ratios between the volumes of primal simplices and their dual cells. In contrast, we propose a Hodge star operator that does not use a dual mesh. Since our dual forms are again located on primal elements, we can compute the wedge product of primal and dual forms, hence define further operators using our discrete Hodge star and polygonal wedge product. However, this primal–primal definition brings some drawbacks as well, we discuss them in Section 3.2.

2.4 The inner product

By employing our proposed discrete wedge product $\wedge$ and Hodge star operator $\star$, we define the inner product matrices by $\mathsf{M} := \wedge\star$, that turns to be identical to the one introduced in [M. and M. 2011, Lemma 3] for the case of product of two 1–forms restricted to a polygon.

2.5 The codifferential

On a Riemannian n–manifold, the Hodge star operator is employed to define the codifferential operator $\delta(\alpha^k) = (-1)^{n(k-1)+1} \star d \star \alpha$. It is a linear operator that maps k–forms to $(k-1)$– forms. On 1–forms it is also called the divergence operator.

A discrete codifferential operator on triangle meshes has been defined e.g. in [K. et al. 2013; M. et al. 2005; N. 2003], all these approaches are equivalent since they use the diagonal approximation of the Hodge star operator. [M. and M. 2011, Section 3] hint at a codifferential of 1–forms on general polygonal meshes. The main difference between these and our codifferentials is in the support domain, see Figures 3 and 4.

2.6 The Laplace operator

In exterior calculus, the Laplace operator is given by $\Delta := \delta d + d\delta$, where δ is the codifferential and d the exterior derivative. The Laplacian is defined in this way also in the classical DEC and we follow

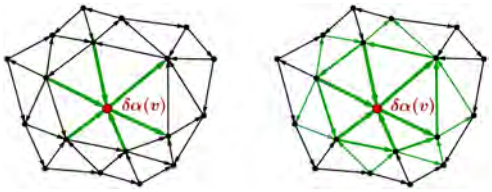

Fig. 3. Comparison of the support domain of the codifferential of 1–forms between the classical DEC (L) and our method (R). The codifferential of a 1–form α is a 0–form located on vertices. The value of $\delta\alpha$ on the red vertex v is a linear combination of values of α on edges colored green. The support domain of our codifferential (R) is larger. The edge thickness reflects the intensity of influence of the corresponding edge values α on $\delta\alpha(v)$.

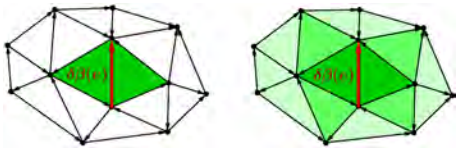

Fig. 4. Comparison of the support domain of the codifferential of 2–forms between the classical DEC (L) and our approach (R). The codifferential of a 2–form β is a 1–form $\delta\beta$ located on edges. The value of $\delta\beta$ on the red edge e is a linear combination of the values of β on faces colored green. The color intensity of faces reflects the intensity of influence on $\delta\beta(e)$.

this convention. The classical Laplacian on 0–forms is also called the *cotan Laplace operator*. Even though many different approaches lead to the cotan–formula, MacNeal [H. 1949] is often considered to be the first to derive it.

Discrete Laplace operators on general polygonal meshes were introduced in [M. and M. 2011]. By Theorem 2 therein, on triangle meshes their polygonal Laplacian of 0–forms reduces to the cotan Laplace operator. In Figure 5 we compare the support domain of our Laplacian to theirs.

2.7 The contraction operator and the Lie derivative

The Lie derivative can be thought of as an extension of a directional derivative of a function to derivative of tensor fields (such as vector fields or differential forms) along a vector field. The Lie derivative is invariant under coordinate transformations, which makes it an appropriate version of a directional derivative on curved manifolds. It evaluates the change of a tensor field along the flow of another vector field and is widely used in mechanics.

Our discretization of Lie derivative of functions (0–forms) corresponds to the functional map framework of [O. et al. 2013], but now generalized to polygonal meshes. Our discrete Lie derivatives are thus linear operators on functions on a manifold that produce new functions, with the property that the derivative of a constant function is 0. Furthermore, both theirs and our Lie bracket of two vector fields (Lie derivative of a vector field wrt a vector field) produces another vector field. However, whereas their framework is build for triangle meshes, we work with general polygonal meshes.

While maintaining the discrete exterior calculus framework, our work can also be interpreted as an extension of the Lie derivative

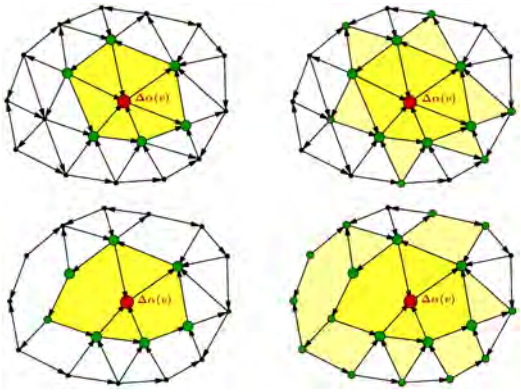

Fig. 5. Comparison of support domains of the Laplacian of 0–forms between the classical DEC on triangle meshes (top left), Laplacian of [M. and M. 2011] for $\lambda = 0$ (bottom left), our Laplacian on triangle (top right) and polygonal (bottom right) meshes. The Laplacian of a 0–form α is a 0–form $\Delta\alpha$ located again on vertices. The value of $\Delta\alpha$ on the red vertex v is a linear combination of values of α on vertices colored green. The support domain of our Laplacian is always larger, the point size reflects the intensity of influence of respective αs on $\Delta\alpha(v)$. We also color yellow the faces whose vertices carry the αs that enter as variables for $\Delta\alpha(v)$.

of 1–forms presented in [P. et al. 2011] from planar regular grids to surface polygonal meshes in space.

3 PRIMAL-TO-PRIMAL OPERATORS

This section contains the actual results of our research – we present the theory and numerical evaluation of each operator and operation, evaluate the quality of our approximations by setting our results against analytical solutions, and also compare the output of our calculations to outputs computed by other DEC schemes.

Not using dual meshes simplifies the definition of several operators on polygonal meshes, which may be a difficult task otherwise. Moreover, it helps to maintain the compatibility of our operators since both the initial and the mapped discrete forms are located on primal elements. However, this approach also brings some drawbacks, we discuss them in this section.

Our framework is an extension of our method that has been studied already in [L. 2017] and presented as a poster in [L. and L. 2017].

3.1 The Discrete Wedge Product

Just like the wedge product of differential forms, our discrete wedge product is a product of two discrete forms of arbitrary degree k and l that returns a form of degree $k + l$ located on primal $(k + l)$–dimensional cells (see Figure 6).

On triangle meshes our discrete wedge product is identical to the cup product given by [H. 1957] and on quadrilaterals it is equivalent to the cubical cup product of [F. 2012]. Further, the wedge product of differential forms satisfies the Leibniz product rule with exterior derivative and is skew–commutative. The discrete wedge product must satisfy these properties as well, we thus appropriately extend the discrete wedge product from triangles and quads to general polygons and derive the following formulas:

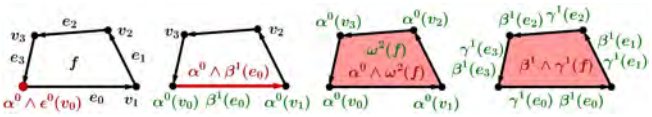

Fig. 6. The wedge product on a quadrilateral: the product of two 0–forms is a 0–form located on vertices (far left). The product of a 0–form with a 1–form is a 1–form located on edges (center left). The product of a 0–form with a 2–form is a 2–form located on faces (center right), and the product of two 1–forms is a 2–form located on faces (far right).

Definition 3.1. *Let S be a surface mesh (pseudomanifold) whose faces (2–cells) are polygons. The polygonal wedge product $\wedge : C^k(S) \times C^l(S) \to C^{k+l}(S)$ of two discrete forms α^k, β^l is a $(k+l)$–form $\alpha^k \wedge \beta^l$ defined on each $(k+l)$–cell $c^{k+l} \in S$. Let $f = (v_0, \ldots, v_{p-1})$ be a p–polygonal face, $e = (v_i, v_j)$ an edge, and v a vertex of S, the **polygonal wedge product** is given for each degree and per each $(k + l)$–cell by:*

$$
\begin{aligned}
(\alpha^0 \wedge \beta^0)(v) &= \alpha(v)\beta(v), \\
(\alpha^0 \wedge \beta^1)(e) &= \frac{1}{2}(\alpha(v_i) + \alpha(v_j))\beta(e), \\
(\alpha^0 \wedge \beta^2)(f) &= \frac{1}{p}\Big(\sum_{i=0}^{p-1} \alpha(v_i)\Big)\beta(f), \\
(\alpha^1 \wedge \beta^1)(f) &= \sum_{a=1}^{\lfloor \frac{p-1}{2} \rfloor} \Big(\frac{1}{2} - \frac{a}{p}\Big) \sum_{i=0}^{p-1} \alpha(i)(\beta(i+a) - \beta(i-a)),
\end{aligned}
$$

where $\alpha(i) := \alpha(e_i)$, $\beta(j) := \beta(e_j)$, and all indices are modulo p.

The polygonal wedge product is illustrated in Figures 2 and 6. It is a bilinear operation that is skew–commutative:

$$\alpha^k \wedge \beta^l = (-1)^{kl} \beta^l \wedge \alpha^k,$$

matching its continuous analog. As premeditated, it satisfies the Leibniz product rule with discrete exterior derivative:

$$d(\alpha^k \wedge \beta^l) = d\alpha \wedge \beta + (-1)^k \alpha \wedge d\beta.$$

Further, the wedge product of three 0–forms is trivially associative (it is equivalent to multiplication of three scalar values). For proofs, see [L. 2017, Proposition 3.2.3].

Unfortunately for higher degree forms it is not associative in general, only if one of the 0–forms involved is constant. This is a common drawback of discrete wedge products, see e.g. [N. 2003, Remark 7.1.4.].

In matrix form, the polygonal wedge product reads:

$$
\begin{aligned}
\alpha^0 \wedge \epsilon^0 &= \alpha^0 \odot \epsilon^0, \\
\alpha^0 \wedge \beta^1 &= (\mathsf{B}\,\alpha^0) \odot \beta^1, \\
\alpha^0 \wedge \omega^2 &= (\mathsf{fv}\,\alpha^0) \odot \omega^2, \\
(\beta^1 \wedge \gamma^1)|_f &= (\beta^1|_f)^\top\, \mathsf{R}(\gamma^1|_f),
\end{aligned}
$$

where $\odot$ is the Hadamard (element–wise) product, $\beta|_f$ denotes the restriction of β to a p–polygonal face f, and the matrices $\mathsf{B} \in$

$\mathbb{R}^{|E|\times|V|}$, $\mathsf{fv} \in \mathbb{R}^{|F|\times|V|}$, and $\mathsf{R} \in \mathbb{R}^{p\times p}$ per f read:

$$\mathsf{B}[i,j] = \begin{cases} \frac{1}{2} & \text{if } v_j \prec e_i, \\ 0 & \text{otherwise.} \end{cases} \tag{1}$$

$$\mathsf{fv}[i,j] = \begin{cases} \frac{1}{p_i} & \text{if } v_j \prec f_i, f_i \text{ is a } p_i\text{–gon}, \\ 0 & \text{otherwise.} \end{cases} \tag{2}$$

$$\mathsf{R} = \sum_{a=1}^{\lfloor \frac{p-1}{2} \rfloor} \left(\frac{1}{2} - \frac{a}{p}\right) \mathsf{R}_a, \tag{3}$$

$$\mathsf{R}_a[k,j] = \begin{cases} 1 & \text{if } e_j \text{ is } (k+a)\text{–th halfedge of } f, [f:e_j] = 1, \\ -1 & \text{if } e_j \text{ is } (k-a)\text{–th halfedge of } f, [f:e_j] = 1, \\ 0 & \text{otherwise.} \end{cases} \tag{4}$$

3.1.1 Numerical evaluation. We perform the numerical evaluation of our polygonal wedge product as an approximation to the continuous wedge product on a given mesh S over a smooth surface in the following fashion:

1. We integrate each differential l–form over all l–dimensional cells of the mesh S and thus define discrete forms α^0, β^1, γ^1, and ω^2:

$$\alpha^0(v) = A(v), \quad \beta^1(e) = \int_e B, \quad \gamma^1(e) = \int_e \Gamma, \quad \omega^2(f) = \int_f \Omega,$$

where Greek capital letters denote the respective continuous differential forms. In practice, we integrate the continuous differential 2–form Ω over a set of triangles (C, v_i, v_{i+1}) that approximate the possibly non–planar face $f = (v_0, \ldots, v_{p-1})$, where C is the centroid of f projected on the given underlying Riemannian surface (that is why we use simple surfaces such as spheres and tori for our tests). See the illustration bellow.

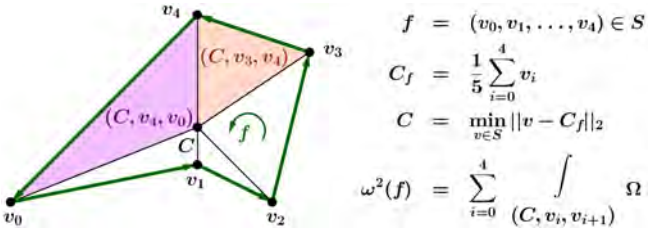

2. Next we compute the polygonal wedge products $(\alpha^0 \wedge \beta^1)(e)$, $(\alpha^0 \wedge \omega^2)(f)$, $(\beta^1 \wedge \gamma^1)(f)$ using our formulas.

3. We also calculate analytical solutions of the (continuous) wedge products and discretize (integrate) these solutions:

$$A \wedge B(e) = \int_e A \wedge B, \quad A \wedge \Omega(f) = \int_f A \wedge \Omega, \quad B \wedge \Gamma(f) = \int_f B \wedge \Gamma.$$

4. We then compute the L^∞ and L^2 errors. So let ξ^k denote our solution (a discrete k–form) and Ξ^k the respective discretized analytical solution, we compute:

$$\mathsf{Error}_2 = \left(\xi^k - \Xi^k\right)^\top M_k \left(\xi^k - \Xi^k\right),$$
$$\mathsf{Error}_\infty = ||\xi^k - \Xi^k||_\infty = \max_{c^k}(|\xi^k(c^k) - \Xi^k(c^k)|),$$

where M_k are discrete L^2 Hodge inner product matrices, concretely, $M_2 \in \mathbb{R}^{|F|\times|R|}$ and $M_0 \in \mathbb{R}^{|V|\times|V|}$ are diagonal matrices given by

$$M_2[i,i] = \frac{1}{|f_i|}, \quad M_0[i,i] = \sum_{f_j \succ v_i} \frac{|f_j|}{p_j}, \tag{5}$$

and M_1 is the inner product of two 1–forms of [M. and M. 2011], i.e., for two 1–forms ϵ and λ, M_1 is defined in the sense that

$$\epsilon^\top M_1 \lambda = \sum_f \epsilon|_f^\top M_f \lambda|_f, \quad M_f := \frac{1}{|f|} B_f B_f^\top, \tag{6}$$

where $\epsilon|_f$ again denotes the restriction of ϵ to a p–polygonal face f and B_f denotes a $p \times 3$ matrix with edge midpoint positions as rows (we take the centroid of each face as the center of coordinates per face).

5. To further evaluate the numerical convergence behavior, we refine the mesh over the given smooth underlying surface. The smooth surfaces used for tests are: unit sphere, torus azimuthally symmetric about the z-axis, and planar square. To create unstructured meshes, we randomly eliminate a given percentage of edges of an initially regular mesh.

We also use **jittering** to evaluate the influence of irregularity of a mesh on the experimental convergence. When jittering, we start with a regular mesh and displace each vertex in a random tangent direction to distance $r \cdot |e|$, where $|e|$ is the shortest edge length, and then project all thus displaced vertices on a given underlying smooth surface.

If not stated otherwise, all graphs use $\log_{10}$ scales on both the horizontal and vertical axes.

We have tested quadratic and trigonometric differential forms on flat and curved surface meshes (with non–planar faces) and our polygonal wedge products exhibit at least linear convergence to the respective analytical solutions, both in L^2 and L^∞ norm. In Figure 7 we give an example.

3.2 The Hodge Star Operator

We define a discrete Hodge star operator as a homomorphism (linear operator) from the group of k–forms to $(2-k)$–forms, i.e. $\star : C^k(S) \to C^{2-k}(S), 0 \le k \le 2$. But since we do not employ any dual mesh and there is no isomorphism between the groups of k– and $(2-k)$–dimensional cells, our Hodge star is not an isomorphism (invertible operator), unlike its continuous counterpart and diagonal approximations for which $\star^{-1}\star$ is the identity.

On the other hand, thanks to the dual forms being located on elements of our primal mesh, we can compute discrete wedge products of primal and dual forms and thus define a discrete inner product and discrete contraction operator later on.

Moreover, thanks to the Hodge star operating on primal meshes, we circumvent the ambiguity of defining dual meshes of unstructured general polygonal meshes. The idea of defining a Hodge star operator without using a dual mesh was borrowed from [F. 2012], where the author suggests metric–independent Hodge star operators on simplicial and cubical complexes.

Our formulas for discrete Hodge star operators are motivated by two conditions:

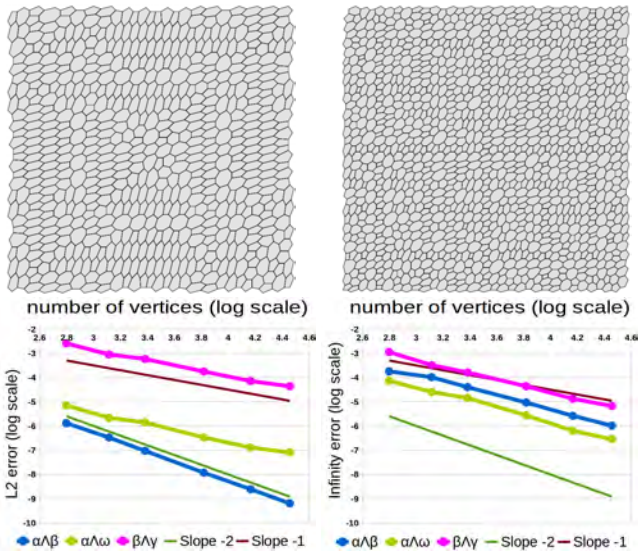

Fig. 7. Convergence of the wedge products on a set of unstructured polygonal meshes on a planar square to analytical solutions in L^2 norm (L) and L^∞ norm (R). Both axes are in $\log_{10}$ scale. The differential forms tested are trigonometric forms $\alpha^0 = \sin(x)\cos(y) + 1$, $\beta^1 = (\sin^2(x) - 1)dx + (3\cos(x+2) + \sin(y))dy$, $\gamma^1 = (\cos(x)\sin(y) + 3)dx + \cos(y)dy$, $\omega^2 = (\sin(xy) + \cos(1))dx \wedge dy$. Above are samples of tested meshes, all over a planar $[-1, 1]^2$ square.

(1) The Hodge dual of constant discrete forms on planar surfaces is exact, thus also $\star\mu = 1$ and $\star 1 = \mu$ just like on Riemannian manifolds, where μ is the volume form on a given Riemannian manifold (for details see [R. et al. 1988, Section 6.5]).
(2) The discrete Hodge star operator on 1–forms leads to the L^2–Hodge inner product on 1–forms identical to the one of [M. and M. 2011, Lemma 3].

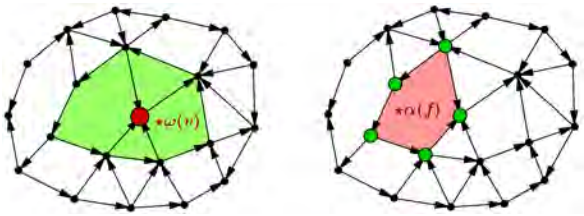

Fig. 8. On the left, the Hodge dual of a 2–form ω is a 0–form $\star\omega$, which value on a vertex v (colored red) is a linear combination of values of ω on adjacent faces (colored green). On the right, the Hodge dual of a 0–form α is a 2–form $\star\alpha$, the value of $\star\alpha$ on a face f (colored red) is a linear combination of values of α on vertices (green) of that face.

The Hodge star operator on 2–forms takes in account the degree p_i of p_i–polygonal faces f_i and their vector areas $|f_i|$. If ω^2 is a 2–form, then the 0–form $\star\omega$ on a vertex v is given by

$$(\star_2\omega)(v) = \frac{1}{\sum\limits_{f_i \succ v} \frac{|f_i|}{p_i}} \cdot \sum_{f_i \succ v} \frac{\omega(f_i)}{p_i}, \tag{7}$$

i.e., it is a linear combination of values of ω on faces adjacent to v, see Figure 8 left.

The Hodge star on an 1–form β^1 is first defined per halfedges of a p–polygonal face f as:

$$\star_1 \beta = \mathsf{W}_1 \mathsf{R}^\top \beta, \tag{8}$$

where R is the matrix defined in (3) and W_1 is a symmetric $p \times p$ matrix given by:

$$\mathsf{W}_1[i,j] = \frac{\langle e_i, e_j \rangle}{|f|},$$

for e_k the halfedges incident to and having the same orientation as the face f, where $\langle ., . \rangle$ denotes the Euclidean dot product.

If an edge e is not on boundary, it has two adjacent faces, thus we compute the values of $\star\beta$ on corresponding halfedges, sum their values with appropriate orientation sign and divide the result by 2, see an example in Figure 9.

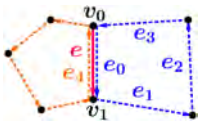

Fig. 9. Let $\beta \in C^1$ and $e = (v_0, v_1)$ be the edge with e_0, e_4 as the corresponding halfedges, then $\star\beta(e) = \frac{\star\beta(e_0) - \star\beta(e_4)}{2}$, where $\star\beta(e_4)$ is a linear combination of values of β on dashed orange edges and $\star\beta(e_0)$ is a linear combination of values of β on dashed blue edges, concretely $\star\beta(e_0) = \frac{1}{4|f_0|}\Big((\langle e_0, e_1\rangle - \langle e_0, e_3\rangle)(\beta(e_0) - \beta(e_2)) + (\langle e_0, e_0\rangle - \langle e_0, e_2\rangle)(\beta(e_3) - \beta(e_1))\Big)$.

The Hodge dual of a 0–form α is a 2–form $\star\alpha$ defined per a p–polygonal face f by:

$$(\star_0\alpha)(f) = \frac{|f|}{p} \sum_{v_i \succ f} \alpha(v_i), \tag{9}$$

and it is simply the arithmetic mean of the values of α on vertices of the given face f multiplied by the vector area $|f|$.

In matrix form, the discrete Hodge star operators read

$$\star_0 = \mathsf{W}_F\, \mathsf{fv},$$
$$\star_1 = \mathsf{A}\, \mathsf{W}_1\, \mathsf{R}^\top,$$
$$\star_2 = \mathsf{W}_V^{-1}\, \mathsf{fv}^\top,$$

where fv and R are defined in equations (2) and (3–4), resp., and $\mathsf{W}_F \in \mathbb{R}^{|F|\times|F|}$, $\mathsf{W}_V \in \mathbb{R}^{|V|\times|V|}$, $\mathsf{A} \in \mathbb{R}^{|E|\times|E|}$ are given by

$$\mathsf{W}_F[i,i] = |f_i|, \quad \mathsf{W}_V[i,i] = \sum_{f_k \succ v_i} \frac{|f_k|}{p_k},$$

$$\mathsf{A}[i,j] = \begin{cases} 1 & \text{if } i = j,\ e_i \text{ is on boundary,} \\ \frac{1}{2} & \text{if } i = j,\ e_i \text{ is not on boundary,} \\ -\frac{1}{2} & \text{if } e_i = -e_j, \\ 0 & \text{otherwise.} \end{cases}$$

Even though our Hodge star matrices are not diagonal, they are highly sparse and thus computationally efficient. We have performed several numerical tests on linear, quadratic, and trigonometric forms on planar and curved meshes and they exhibit the same (at least linear) convergence rate. We give an example in Figure 10.

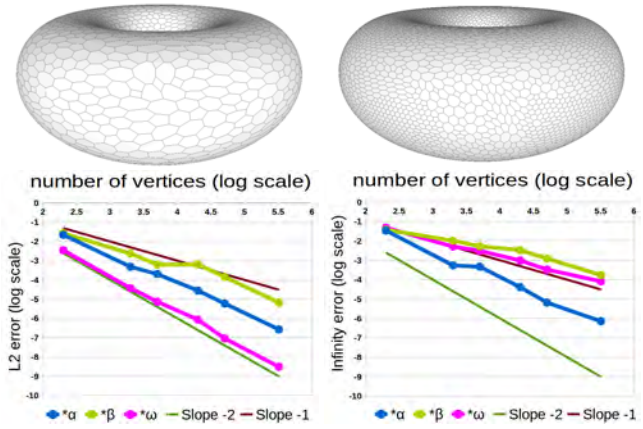

Fig. 10. In the top row we show two meshes of a torus azimuthally symmetric about the z-axis with 5k vertices (L) and 20k vertices (R). Bellow are graphs showing the approximation errors of the discrete Hodge star on a set of such irregular polygonal meshes on the torus, in L^2 norm (L) and L^∞ norm (R). We have chosen $\alpha^0 = x^2 + y^2$, $\beta^1 = \mathbb{X}^\flat$, where $\mathbb{X} = (-y, x, 0)$ is a tangent vector field, and $\omega^2 = \mu$ is the area element on the torus. Thus $\star\mu = 1$, $\star\alpha = (x^2+y^2)\mu$, and $\star\beta = \mathbb{Y}^\flat$, where $\mathbb{Y} = 2(-xz, -yz, x^2+y^2-\sqrt{x^2+y^2})$ is a tangent vector field orthogonal to $\mathbb{X}$. Both axes are in $\log_{10}$ scale.

3.3 The Hodge Inner Product

The L^2–Hodge inner product of differential forms $\alpha, \beta \in \Omega^k(M)$ on a Riemannian manifold M is defined as:

$$(\alpha^k, \beta^k) := \int_M \alpha \wedge \star\beta.$$

We define a **discrete L^2–Hodge inner product** on a mesh S by:

$$(\alpha^k, \beta^k) := \sum_{f \in S} \big(\alpha \wedge \star\beta\big)(f) = \alpha^\top \mathsf{M}_k\, \beta,\ k = 0, 1, 2,$$

where M_k are the discrete Hodge inner product matrices that read:

$$\begin{aligned} \mathsf{M}_0 &= \mathsf{fv}^\top \mathsf{W}_F\, \mathsf{fv}, \\ \mathsf{M}_1 &= \mathsf{R}\, \mathsf{A}\, \mathsf{W}_1\, \mathsf{R}^\top, \\ \mathsf{M}_2 &= \mathsf{fv}\, \mathsf{W}_V^{-1}\, \mathsf{fv}^\top. \end{aligned}$$

It can be shown that our inner product of 1–forms restricted to a face f is identical to the one of [M. and M. 2011, Lemma 3]: $\mathsf{R}\,\mathsf{W}_1\,\mathsf{R}^\top|_f = \frac{1}{|f|} B_f B_f^\top$, where B_f is a $\mathbb{R}^{p\times 3}$ matrix with edge midpoint vectors as rows (we take the centroid of each p–face f as the center of origin per face). However, if a given mesh S is not just a single face they differ in general, i.e., for 1–forms β^1, γ^1:

$$\beta^\top \mathsf{M}_1\, \gamma = \beta^\top \mathsf{R}\,\mathsf{A}\,\mathsf{W}_1\,\mathsf{R}^\top \gamma \ \neq\ \beta^\top \mathsf{R}\,\mathsf{W}_1\,\mathsf{R}^\top \gamma = \sum_{f\in S} \beta^\top \frac{1}{|f|} B_f B_f^\top \gamma.$$

To numerically evaluate our inner products, we calculate discrete L^2–Hodge norms of forms $\alpha^0, \beta^1, \omega^2$ over a mesh S and compare them to their respective analytical L^2 norms. That is, if Γ^k is a differential k–form and γ^k the corresponding discrete k–form, we compute the error of approximation as:

$$\int_S \Gamma \wedge \star\Gamma - \sum_{f\in S} \gamma \wedge \star\gamma = \int_S \Gamma \wedge \star\Gamma - \gamma^\top \mathsf{M}_k\, \gamma.$$

An example of numerical evaluation of our L^2–Hodge inner products and numerical evaluation of inner products M_0 and M_1 of [M. and M. 2011], see also the equations (5 – 6), is given in Figure 11. The experimental convergence rate of our discrete L^2 norms is at least linear on all tested forms on compact manifolds with or without boundary.

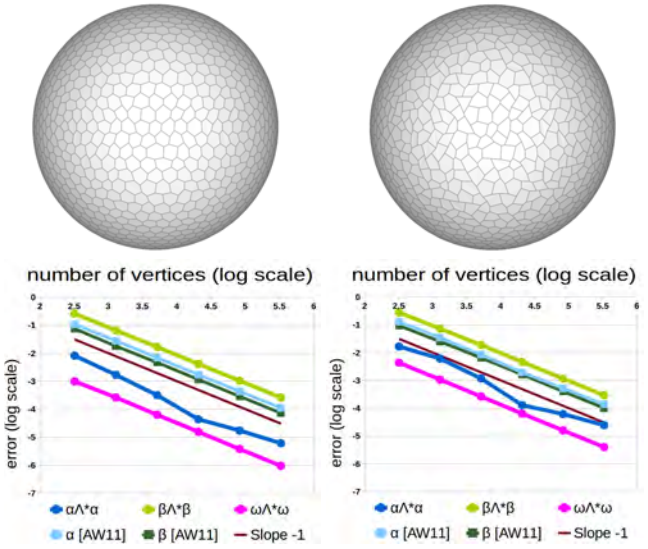

Fig. 11. The influence of jittering on experimental convergence of discrete L^2–Hodge inner norms to respective analytically computed solutions. The graph on the left illustrates experimental convergence on a set of jittered meshes with $r = 0.2$ and sample mesh with 5k vertices is located above. Analogically on the right, with $r = 0.4$. We have chosen $\alpha^0 = x^2 + y^2$, $\beta^1 = -xzdx - yzdy + (x^2+y^2)dz$, $\omega^2 = xdy \wedge dz + ydz \wedge dx + zdx \wedge dy$. Here $\alpha \wedge \star\alpha$ denotes our L^2–Hodge inner product norm on 0–form α, and similarly for β and γ. α [AW11] denotes the inner products of 0–forms and β [AW11] the product of 1–forms of [M. and M. 2011].

3.4 The Contraction Operator

The contraction operator $\mathbf{i}_X$, also called the interior product, is the map that sends a k–form ω to a $(k-1)$–form $\mathbf{i}_X\,\omega$ such that

$$(\mathbf{i}_X\,\omega)(X_1, \ldots, X_{k-1}) = \omega(X, X_1, \ldots, X_{k-1})$$

for any vector fields $X_1, \ldots, X_{k-1}$. The following property holds [N. 2003, Lemma 8.2.1]:

Lemma 3.1. *Let M be a Riemannian n–manifold, $X \in \mathfrak{X}(M)$ a vector field, then for the contraction of a differential k–form α with a vector field X holds:*

$$i_X\alpha = (-1)^{k(n-k)} \star (\star\alpha \wedge X^\flat),$$

where $\flat : \mathfrak{X}(M) \to \Omega(M)$ *is the flat operator.*

Since we already have discrete wedge and Hodge star operators that are compatible with each other, we can employ the lemma to define our **discrete contraction operator** $\mathbf{i}_X : C^k(S) \to C^{k-1}(S)$ on a polygonal mesh S by:

$$\mathbf{i}_X\, \alpha = (-1)^{k(2-k)} \star (\star\alpha \wedge X^\flat), \quad \alpha \in C^k(S),\ k = 1, 2, \tag{10}$$

where the **discrete flat operator** on a vector field X is given by discretizing its value over all edges of S. Let $e = (v_0, v_1)$ be an edge of S, then $e = e(t) = v_0 + (v_1 - v_0)t, t \in [0, 1]$, and we set:

$$X^\flat(e) = \int_e \langle e', X\rangle = \int_0^1 \langle e'(t), X(e(t))\rangle dt. \tag{11}$$

Thus the discrete contraction operator is a linear operator that maps k–forms located on k–dimensional primal cells to $(k-1)$–forms located on $(k-1)$–dimensional primal cells.

Our discrete contraction of differential 2–forms wrt to different vector fields exhibit linear convergence to the analytically computed solutions, both in L^∞ and L^2 norms. On 1–forms, the errors of approximation decrease linearly in L^2 norm and with slope 0.5 in L^∞ norm, see two examples in Figure 12.

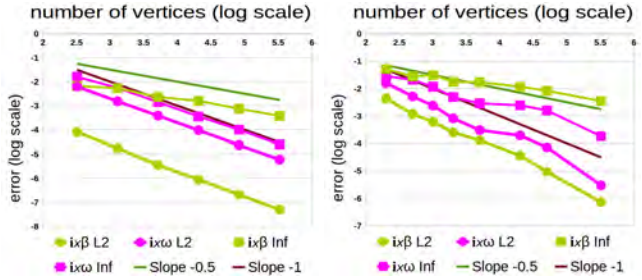

Fig. 12. The contraction operator on a unit sphere (L) and a torus (R). For the sphere we have used the set of jittered with $r = 0.4$ as in Figure 11, and contracted the same forms as therein wrt vector field $X = (-y, x, 0)$. For the torus (R) we have contracted the differential forms of Figure 10 wrt vector field $X = 2(-xz, -yz, x^2 + y^2 - \sqrt{x^2 + y^2})$ on the same set of meshes as therein. $\mathbf{i}_X\, \beta$ L2 denotes the L^2 error approximation of the contraction operator on the 1–form β, whereas $\mathbf{i}_X\, \beta$ Inf denotes the L^∞ error approximation on β, and similarly for the 2–form ω.

3.5 The Lie Derivative

We define the **discrete Lie derivative** $\mathsf{L}_X : C^k(S) \to C^k(S)$ using the Cartan's magic formula and our discrete contraction operator:

$$\mathsf{L}_X\, \alpha = \mathbf{i}_X\, d\alpha + d\, \mathbf{i}_X\, \alpha,\ \alpha \in C^k(S),\ k = 0, 1, 2. \tag{12}$$

Unfortunately, the Leibniz product rule of the contraction operator and Lie derivative with discrete exterior derivative is not satisfied in general. Concretely

$$\begin{aligned} \mathbf{i}_X(\alpha^k \wedge \beta^l) &= (\mathbf{i}_X\, \alpha^k) \wedge \beta^l + (-1)^k \alpha^k \wedge (\mathbf{i}_X\, \beta^l), \\ \mathsf{L}_X(\alpha^k \wedge \beta^l) &= (\mathsf{L}_X\, \alpha^k) \wedge \beta^l + \alpha^k \wedge (\mathsf{L}_X\, \beta^l), \end{aligned}$$

holds only if α or β is a closed 0–form. Already in [N. 2003] the author noticed that the Leibniz rule for Lie derivative might not hold due to the discrete wedge product not being associative in general. We confirm the observation in [M. et al. 2005] that the Leibniz rule may be satisfied only for closed forms.

The Lie derivatives exhibit converging behavior on all tested forms on regular meshes, planar and non–planar. However, the L^2 error of approximation of Lie derivatives of 1– and 2–forms on irregular meshes stays rather constant, see an example on a set of regular versus jittered meshes on a unit sphere in Figure 13. In this figure we can see that the L^2 error of the Lie derivative of a 1–form β and a 2–form ω on regular meshes decreases with slope -0.5, whereas on very irregular meshes it stays constant (Fig. 13 top left).

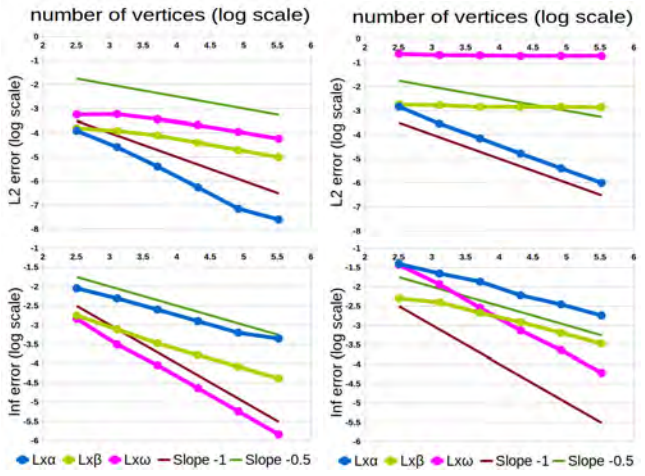

Fig. 13. The influence of jittering on experimental convergence of discrete Lie derivatives on a set of regular polygonal meshes on a sphere (L) and a set of jittered meshes with vertex displacement by 0.4× shortest edge length (R) – we use the same set of jittered meshes as in Figure 11. In the top row we plot the errors in L^2 norms and bellow in L^∞ norm ($\log_{10}$ scales). We use the same forms and a vector field on the unit sphere as in Figure 12.

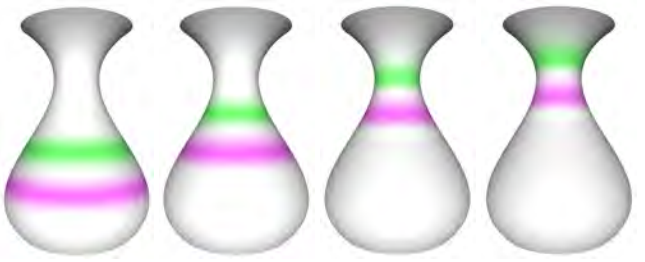

Fig. 14. Lie derivative used for advection of a color function (left). We encode the function as a 0–form β and advect it using equation (19). The advected function after 2000 iterations (center left), 4000 (center right), and 5000 iterations (right) with time step 10^{-2}.

3.6 The Codifferential Operator

Just like the codifferential on a Riemannian n–manifold, we define our **discrete codifferential operator** on a k-form β, $k > 0$, by

$$\delta_k \beta^k = (-1)^{n(k-1)+1} \star d \star \beta.$$

Thus in matrix form our codifferential operators read:

$$\delta_1 = -\,\mathrm{W}_V^{-1}\,\mathrm{fv}^\top\; d_1\; \mathrm{A}\,\mathrm{W}_1\,\mathrm{R}^\top,$$
$$\delta_2 = -\,\mathrm{A}\,\mathrm{W}_1\,\mathrm{R}^\top\; d_0\; \mathrm{W}_V^{-1}\,\mathrm{fv}^\top.$$

If M is a compact manifold without boundary or if α or $\star\beta$ has zero boundary values, then the codifferential is the adjoint operator of the exterior derivative with respect to the L^2–Hodge inner product:

$$(d\alpha, \beta) = (\alpha, \delta\beta) \quad \forall \alpha \in \Omega^{k-1}(M), \beta \in \Omega^k(M). \tag{13}$$

[M. and M. 2011] use this equation (13) to derive their discrete codifferential operator on 1–forms by:

$$\begin{aligned}(\delta_1\alpha, \beta) &= (\alpha, d_0\beta) \;\text{ for } \alpha \in C^1, \beta \in C^0\\ (\delta_1\alpha)^\top M_0\beta &= \alpha^\top M_1 d_0\beta\\ \alpha^\top\delta_1^\top M_0\beta &= \alpha^\top M_1 d_0\beta\\ \delta_1^\top M_0 &= M_1 d_0\\ \delta_1 &= (M_1 d_0 M_0^{-1})^\top = M_0^{-1} d_0^\top M_1,\end{aligned}$$

where M_0 and M_1 are as in equations (5–6). This codifferential reduces to the classical codifferential (e.g. [K. et al. 2013]) in the case of a pure triangle mesh.

To compare the support domain of our and the classical DEC codifferentials, see Figures 3 and 4. In Figure 15 we numerically evaluate our discretization and compare it to the codifferential of 1–forms of [M. and M. 2011]. In this example we choose trigonometric forms but the convergence behavior for linear and quadratic forms is the same.

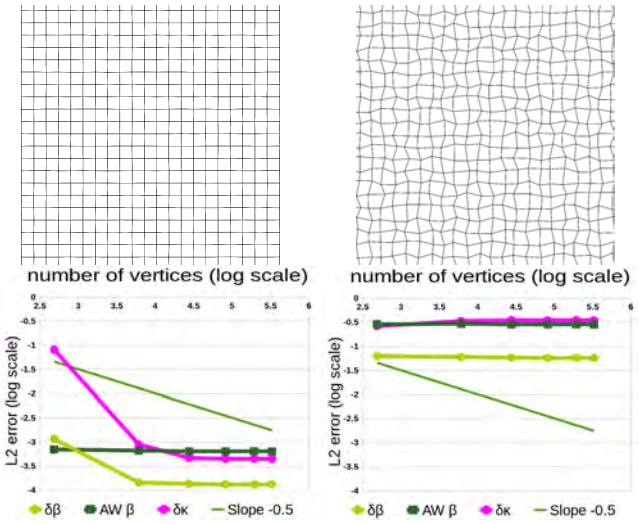

Fig. 15. The influence of jittering on experimental convergence of codifferentials of a 1–form $\beta^1 = (\sin(2x) + \cos(\frac{1}{2}))dx + (3\sin(x) - \cos(y))dy$ and a 2–form $\kappa^2 = (sin(\frac{x+1}{4}) + cos(1 - \frac{y}{3}))dx \wedge dy$ on a set of planar quadrilateral jittered meshes with vertex displacement $0.01\times$ shortest edge length (L) and $0.2\times$ shortest edge length (R). Here $\delta\beta$ denotes the L^2 error of approximation of our codifferential of β to the exact, i.e. analytically computed, solution, AWβ stands for the L^2 error of the codifferential of 1–forms of [M. and M. 2011], $\delta\kappa$ is the L^2 error of our codifferential of the 2–form κ.

3.7 Discrete Laplacians

Laplace–deRham operator Δ is an operator taking differential k–forms to k–forms and is defined as

$$\Delta = d\delta + \delta d, \tag{14}$$

where δ is the codifferential operator and d is the exterior derivative. We define our discrete Laplacian in the same manner, using the codifferentials presented in the previous section. On 0–forms (functions), it simplifies to $\Delta = \delta d$.

Our Laplace operator on 0–forms is linearly precise, i.e., it is zero on linear forms in the plane. In Figure 16 we depict experimental convergence of our discrete Laplacian on trigonometric 0–forms and we compare it to the discrete Laplacian on general polygonal meshes of [M. and M. 2011] on two sets of jittered meshes. The experimental convergence behavior observed is the same for other kinds of 0–forms.

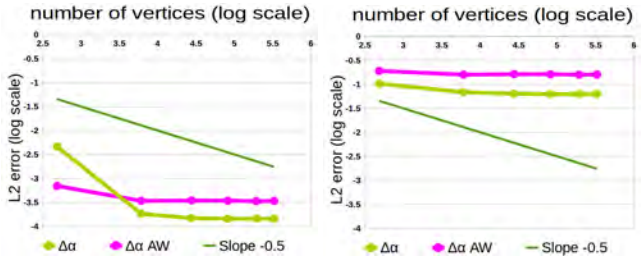

Fig. 16. The discrete Laplacian operator of a trigonometric 0–form $\alpha^0 = sin(x-1) - cos(2y)$ on two sets of jittered quadrilateral planar meshes, with displacement $r = 0.01$ (L) and $r = 0.2$ (R). We use the same set of meshes as in Figure 15. $\Delta\alpha$ denotes our Laplacian and $\Delta\alpha$ AW the Laplacian of [M. and M. 2011].

4 APPLICATIONS

In this section we show some basic applications of our operators on general polygonal meshes.

4.1 Implicit Mean Curvature Flow

One of the widely used methods for smoothing a surface is the implicit mean curvature flow. If f is a discrete 0–form representing vertex positions, then Δf give us the direction and magnitude in which we should move each point in order to smooth the given mesh, see e.g. [K. et al. 2013, Section 6.6].

Let f_0 denote the initial state and f_t the configuration after a mean curvature flow of some duration $t > 0$. We employ the *backward Euler scheme* to calculate f_t by solving the linear system:

$$(I - t\Delta)f_t = f_0,$$

where I is the identity matrix. To solve this system, we use the `mldivide` algorithm of MATLAB.

In Figures 1 and 17 we show smoothing of general polygonal meshes and compare our method to the one of [M. and M. 2011] for various parameters λ that can be used to improve their results. After testing also other meshes and several other parameters λ, time steps, and number of iterations, we conclude that our results are

Publication date: August 2018.

visually comparable to the ones smoothed by method of [M. and M. 2011] with $\lambda \in [1, 2]$, and that our scheme does not create as many undesirable artifacts as theirs for $\lambda = 0$.

Fig. 17. Ears of Standford bunny (15k vertices) after applying our Laplacian flow (L), Laplacian flow of [M. and M. 2011] with $\lambda = 0$ (C) and with $\lambda = 2$ (R). We applied 100 iterations with time step $t = 10^{-5}$. There appear degenerate polygons for $\lambda = 0$ (C).

4.2 Helmholtz–Hodge Decomposition

By the Hodge Decomposition Theorem (see e.g. [R. et al. 1988, Theorem 7.5.3]), if M is a compact oriented Riemannian manifold without boundary and $\omega^k \in \Omega^k(M)$, then there exists a $(k-1)$–form α, $(k+1)$–form β, and a harmonic k–form γ (γ is harmonic iff $\Delta\gamma = 0$) such that

$$\omega = d\alpha + \delta\beta + \gamma. \tag{15}$$

Furthermore, $d\alpha$, $\delta\beta$, and γ are uniquely determined.

If instead of forms, we think about a sufficiently smooth vector field $X = (\omega^1)^\sharp$, where $\sharp$ is the sharp operator, then an analogous Helmholtz theorem states that any vector field X can be decomposed into an irrotational vector field (corresponding to $d\alpha$), a divergence–free component (analogous to $\delta\beta$), and a both irrotational and divergence–free vector field (corresponding to γ). Thus the equation (15) is also referred to as to Helmholtz–Hodge decomposition (HHD).

If X is a divergence–free vector field (also known as solenoidal), we can find its so called two–component HHD, i.e., decompose X into a rotational and irrotational part. In terms of differential forms, for $\omega^1 = X^\flat$ we get

$$\omega = \delta\beta + \gamma, \tag{16}$$

where γ is a harmonic 1–form and thus $\gamma^\sharp$ is an irrotational vector field, and $(\delta\beta)^\sharp$ is a rotational vector field. The two–component HHD is used for decomposition of vector fields of incompressible flows.

We use our codifferential operator to find our **discrete two–component Helmholtz–Hodge decomposition** as in equation (16) by performing these steps:

(1) Discretize a given vector field X with discrete flat operator (11) and define discrete 1–form $\omega^1 = X^\flat$.
(2) Find the 2–form β by solving equation $d\delta\beta = d\omega$.
(3) Set $\gamma = \omega - \delta\beta$.

We can then map the discrete 1–forms $\delta\beta$ and γ to discrete vector fields by applying **discrete sharp operator** $\sharp$ defined on an 1–form ϵ and per a vertex v by:

$$\epsilon^\sharp(v) = \frac{1}{\rho(v)} \sum_{f \succ v} \left(\frac{\epsilon(e_2)}{|e_2|} \frac{n_f \times e_1}{|e_1|} - \frac{\epsilon(e_1)}{|e_1|} \frac{n_f \times e_2}{|e_2|} \right), \tag{17}$$

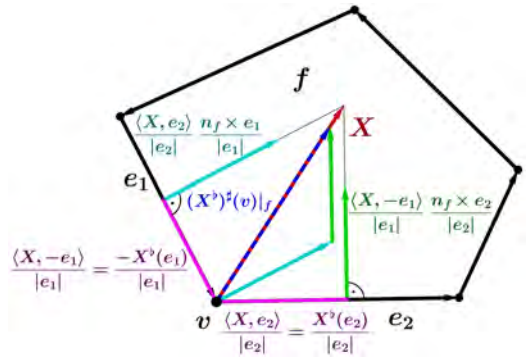

Fig. 18. The discrete sharp operator on a vertex v restricted to a face f. Let $X^\flat$ be a 1–from computed by applying a discrete flat operator on a constant vector field X, then the orthogonal projection of X on the unit direction vector of the edge e_1 equals $\frac{\langle X, e_1\rangle}{|e_1|} = \frac{X^\flat(e_1)}{|e_1|}$. Similarly the orthogonal projection of X on the unit direction vector of e_2 is $\frac{\langle X, e_2\rangle}{|e_2|} = \frac{X^\flat(e_2)}{|e_2|}$. Reconstructing the vector field X from $X^\flat$, i.e., applying the sharp operator on $X^\flat$ as in equation (17), yields vector $(X^\flat)^\sharp|_f = \frac{\langle X, e_2\rangle}{|e_2|}\frac{n_f \times e_1}{|e_1|} - \frac{\langle X, e_1\rangle}{|e_1|}\frac{n_f \times e_2}{|e_2|}$ that has the same direction as X and approximates its magnitude.

where $\rho(v)$ is the number of faces adjacent to v. Further $e_1, e_2 \prec f$, e_1 is the edge which endpoint is v, e_2 is the edge with v as the starting point, see Figure 18, and n_f is a unit normal vector of the face $f = (v_0, \ldots, v_{n-1})$ computed as:

$$n_f = \frac{\hat{n}_f}{|\hat{n}_f|}, \quad \hat{n}_f = \frac{1}{2} \sum_{j=0}^{n-1} (v_j \times v_{j+1}), \text{ indices modulo } n.$$

In Figure 19 we give an example of our HHD of an incompressible vector field on a general polygonal mesh of a torus. In Figure 20 we then employ the HHD to remove vortices of an arbitrary vector field.

4.3 Lie Advection

The Lie derivative finds its application in dynamical systems. In computer graphics the Lie advection of differential forms (including scalar and vector fields) is used for tasks ranging from fluid flow simulation [A. 2007] to authalic parametrization of surfaces [G. et al. 2011].

In Figure 21 we employ our discrete Lie derivative to perform a simple discrete Lie advection of a tangent vector field Y discretized as a 1–form $\beta^1 = Y^\flat$ by a tangent vector field $X = (-y, x, 0)$ on a torus azimuthally symmetric about the z axis. Y is a vorticial vector field given as

$$Y = -\nabla \exp\left(-\left(x + \frac{\sqrt{2}}{2}\right)^2 - \left(y - \frac{\sqrt{2}}{2}\right)^2 - \left(z - \frac{1}{2}\right)^2 \right) \times n, \tag{18}$$

where n is the unit normal vector of the torus. To advect the 1–form β by the flow of X, we discretize β and store its values on edges of the mesh, as usual, and denote this initial state as β_0. We then iterate over our discrete solutions using a simple forward Euler method:

$$\beta_{k+1} = \beta_k - t\, \mathsf{L}_X\, \beta_k, \; k = 0, \ldots, \tag{19}$$

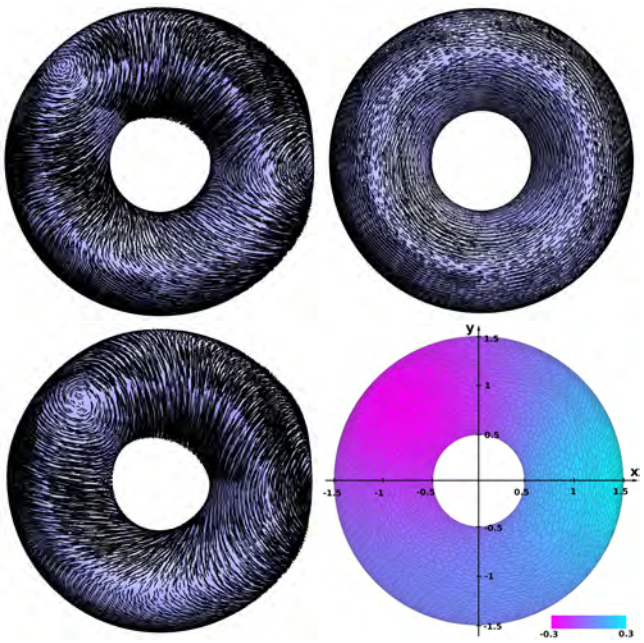

Fig. 19. HHD of a solenoidal vector field X on a torus azimuthally symmetric about the z axis and centered at the origin (a general polygonal mesh with 20k vertices). The decomposed vector field is $X = X_H + X_R$, where $X_H = (-y, x, 0)$ is a harmonic field on the torus, and X_R is a rotational vector field given by $X_R = \nabla(\exp(-(x-x_1)^2-(y-y_1)^2-(z-z_1)^2)-\exp(-(x-x_2)^2-(y-y_2)^2-(z-z_2)^2))\times n$, where n is the unit normal vector of the torus. We have chosen the center of CCW rotation $(x_1, y_1, z_1) = (\frac{3}{2}, 0, 0)$, where the vector potential $\beta^\sharp$ reaches its maximum, and the center of CW rotation at $(x_2, y_2, z_2) = (\frac{-\sqrt{2}}{2}, \frac{\sqrt{2}}{2}, \frac{1}{2})$, where the vector potential $\beta^\sharp$ has its minimum (is negative). Our discrete decomposition gives approximate expected results. In the top left corner is the original vector field X, the harmonic part $\gamma^\sharp$ is shown in the top right, in the bottom left is the rotational part $(\delta\beta)^\sharp$. In the bottom right we also depict the vector potential $\beta^\sharp$, computed by our algorithm, in pseudocolors varying approximately from -0.3 to 0.3.

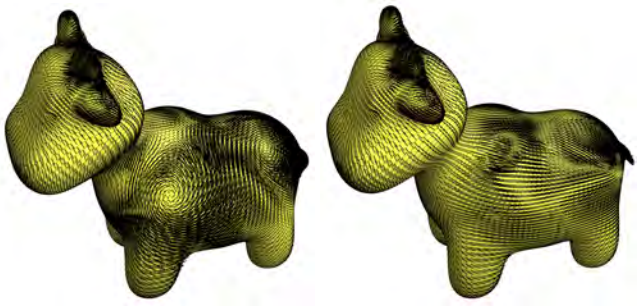

Fig. 20. HHD applied to remove the vortices of a vector field ω on a mesh of Spot (model created by Keenan Crane). On the left is the original vector field $\omega = \delta\beta + \phi$, on the right is its curl–free part ϕ.

where t is the time step, k is the number of iterations, and each $\mathsf{L}_X\,\beta_k$ is computed using our discrete Lie derivative (12). Note that the vector field X is also discretized as a discrete 1–form and its values are stored on edges of the mesh.

The Lie derivative can be employed also for advection of a function by a vector field. In Figure 14 we advect a color function on a mesh of a vase.

5 FUTURE WORK

Applying our operators in geometry processing tasks is a work in progress. E.g., design of tangent vector fields on general polygonal meshes using HHD or vector field processing with Lie derivative is an object of our ongoing research.

Further, we know that it is possible to define a discrete wedge product on tetrahedrons and 3–dimensional (topological) cubes in a way that it satisfies the defining properties of a wedge product such as the bilinearity, Leibniz product rule, and skew–commutativity. Therefore we want to examine the possibility to extend the calculus we have just presented from 2–dimensional to (intrinsically) 3–dimensional manifolds, that is:

- Define DEC operators on 3–dimensional cubical and simplicial complexes, these shall include except the discrete wedge product also the Hodge star operator. Once defined these, we could derive a discrete contraction operator, a Lie derivative, codifferential, and Laplacian, just as we did in the 2–dimensional case.
- Look for a definition of a discrete wedge product on general 3–dimensional polytopes other than tetrahedras and cubes or at least find a subset of polytopes that allow for such a wedge product that would satisfy the Leibniz product rule and other properties. Then possibly follow the workflow above.

6 CONCLUSION

Geometry processing with polygonal meshes is a new developing area, maybe one of the first steps and also the most influential ones has been the definition of discrete Laplacians on general polygonal meshes by [M. and M. 2011]. Our objective was to continue in this venue by presenting a novel discretization of several operators and operations that act directly on general polygonal meshes and are compatible with each other. We thus extend further the DEC framework from simplicial and cubical setting to general polygonal case.

Our aim has been to give a concise yet complete exposition of a primal–primal discrete exterior calculus on general polygonal meshes, including rigorous theory but also simple practical examples. Furthermore, we have tested and discussed empirical convergence of our schemes on regular vs. irregular planar and curved meshes. We have then shown applicability of our approach on several tasks, ranging from Helmholtz–Hodge decomposition to Lie Advection.

We believe that the generality of our framework will make it a useful tool in many geometry processing tasks and will inspire further research in the area.

REFERENCES

McKenzie A. 2007. *HOLA: A High-Order Lie Advection of Discrete Differential Forms, with Applications in Fluid Dynamics.* Master's thesis. California Institute of Technology. Division of Engineering and Applied Science.

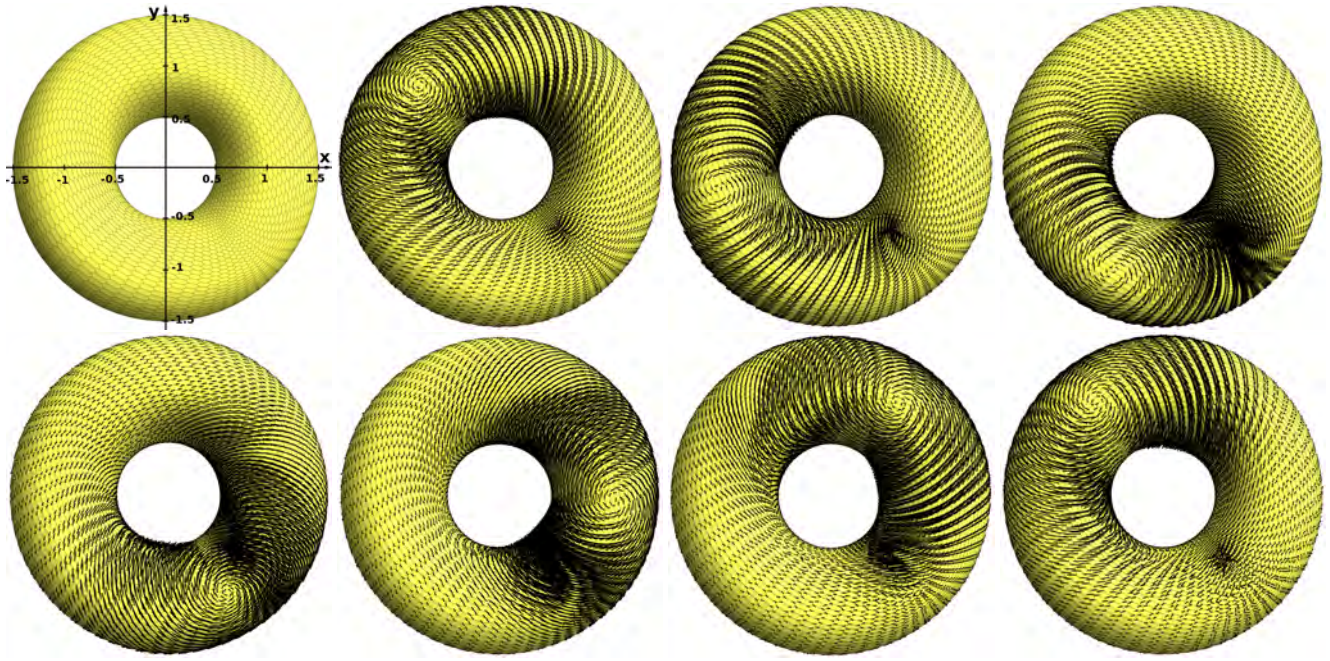

Fig. 21. The Lie advection on a regular polygonal mesh of a torus (8k vertices), the underlying mesh is shown in the top left corner. We advect a 1–form $\beta = Y^\flat$ along the flow of a tangent vector field $X = (-y, x, 0)$, where Y is given in equation (18). The second picture from the left depicts $\beta_0^\sharp$. We apply time steps of length 10^{-3}. From left to right and top to bottom, we plot $Y = \beta_k^\sharp$ after 1000, 2000,..., 5000 iterations. At the bottom right we see $\beta_k^\sharp$ for $k = 6283$. Because the domain is periodic, β should be advected back to its original state β_0 after $2\pi \cdot 10^3 \approx 6283$ iterations. We can see that $\beta_{6283}^\sharp$ gets close to $\beta_0^\sharp$, but some undesirable artifacts appear – especially at the small irregularity around the spot with coordinate position $(\frac{\sqrt{2}}{2}, -\frac{\sqrt{2}}{2}, \frac{1}{2})$.

Arnold R. F. 2012. *The Discrete Hodge Star Operator and Poincaré Duality.* Ph.D. Dissertation. Virginia Polytechnic Institute and State University.

Zou G., Hu J., Gu X., and Hua J. 2011. Authalic Parameterization of General Surfaces Using Lie Advection. *IEEE Transactions on Visualization and Computer Graphics* 17, 12 (Dec. 2011), 2005–2014.

MacNeal R. H. 1949. *The solution of partial differential equations by means of electrical networks.* Ph.D. Dissertation. Pasadena, CA, USA.

Whitney H. 1957. *Geometric Integration Theory.* Princeton University Press.

Crane K., de Goes F., Desbrun M., and Schröder P. 2013. Digital Geometry Processing with Discrete Exterior Calculus. In *ACM SIGGRAPH 2013 Courses (SIGGRAPH '13).* ACM, New York, NY, USA, Article 7, 126 pages. https://doi.org/10.1145/2504435.2504442

Ptackova L. 2017. *A Discrete Wedge Product on Polygonal Pseudomanifolds.* Ph.D. Dissertation. Rio de Janeiro, Brasil.

Ptackova L. and Velho L. 2017. A Primal-to-Primal Discretization of Exterior Calculus on Polygonal Meshes. In *Symposium on Geometry Processing 2017- Posters.* The Eurographics Association. https://doi.org/10.2312/sgp.20171204

Alexa M. and Wardetzky M. 2011. Discrete Laplacians on General Polygonal Meshes. In *ACM SIGGRAPH 2011 Papers (SIGGRAPH '11).* ACM, New York, NY, USA, Article 102, 10 pages. https://doi.org/10.1145/1964921.1964997

Desbrun M., Kanso E., and Tong Y. 2006. Discrete Differential Forms for Computational Modeling. In *ACM SIGGRAPH 2006 Courses (SIGGRAPH '06).* ACM, New York, NY, USA, 39–54. https://doi.org/10.1145/1185657.1185665

Desbrun M., Hirani A. N., Leok M., and Marsden J. E. 2005. Discrete Exterior Calculus. (2005). http://arXiv.org/math.DG/0508341 preprint.

William S. Massey. 1991. *A Basic Course in Algebraic Topology.* Springer New York.

Hirani A. N. 2003. *Discrete Exterior Calculus.* Ph.D. Dissertation. Pasadena, CA, USA. Advisor(s) Marsden, Jerrold E. AAI3086864.

Azencot O., Ben-Chen M., Chazal F., and Ovsjanikov M. 2013. An Operator Approach to Tangent Vector Field Processing. In *Proceedings of the Eleventh Eurographics/ACMSIGGRAPH Symposium on Geometry Processing (SGP '13).* Eurographics Association, Aire-la-Ville, Switzerland, Switzerland, 73–82. https://doi.org/10.1111/cgf.12174

Mullen P., McKenzie A., Pavlov D., Durant L., Tong Y., Kanso E., Marsden J. E., and Desbrun M. 2011. Discrete Lie Advection of Differential Forms. *Found. Comput. Math.* 11, 2 (April 2011), 131–149. https://doi.org/10.1007/s10208-010-9076-y

Abraham R., Marsden J. E., and Ratiu T. 1988. *Manifolds, Tensor Analysis, and Applications: 2Nd Edition.* Springer-Verlag New York, Inc., New York, NY, USA.

Gonzalez-Diaz R., Jimenez M. J., and Medrano B. 2011a. Cubical cohomology ring of 3D photographs. *International Journal of Imaging Systems and Technology* 21, 1 (2011), 76–85. https://doi.org/10.1002/ima.20271

Gonzalez-Diaz R., Lamar J., and Umble R. 2011b. *Cup Products on Polyhedral Approximations of 3D Digital Images.* Springer Berlin Heidelberg, Berlin, Heidelberg, 107–119. https://doi.org/10.1007/978-3-642-21073-0_12

Gu X. and Yau S.-T. 2003. Global Conformal Surface Parameterization. In *Proceedings of the 2003 Eurographics/ACM SIGGRAPH Symposium on Geometry Processing (SGP '03).* Eurographics Association, Aire-la-Ville, Switzerland, Switzerland, 127–137. http://dl.acm.org/citation.cfm?id=882370.882388